Atmos. Chem. Phys. Discuss., 10, 19939–19980, 2010
www.atmos-chem-phys-discuss.net/10/19939/2010/
doi:10.5194/acpd-10-19939-2010

Atmospheric Chemistry and Physics Discussions

Time-resolved measurements of black carbon light absorption enhancement in urban and near-urban locations of Southern Ontario, Canada

T. W. Chan[1], J. R. Brook[2], G. J. Smallwood[3], and G. Lu[2]

[1]ASTB/STB Environment Canada, 335 River Road South, Ottawa, Ontario, K1V 0H3, Canada
[2]ASTB/STB Environment Canada, 4905 Dufferin Street, Toronto, Ontario, M3H 5T4, Canada
[3]National Research Council Canada, 1200 Montreal Road, Ottawa, Ontario, K1A 0R6, Canada

Received: 13 August 2010 – Accepted: 16 August 2010 – Published: 24 August 2010

Correspondence to: T. W. Chan (tak.chan@ec.gc.ca)

Published by Copernicus Publications on behalf of the European Geosciences Union.

Abstract

In this study a photoacoustic spectrometer (PA), a laser-induced incandescence instrument system (LII) and an aerosol mass spectrometer were operated in parallel for in situ measurements of black carbon (BC) light absorption enhancement. Results of a thermodenuder experiment using ambient particles in Toronto are presented first to show that LII measurements of BC are not influenced by particle coating while the PA response is enhanced and also that the nature of this enhancement is influenced by particle morphology. Comparisons of ambient PA and LII measurements at four different locations (suburban Toronto; a street canyon with heavy diesel bus traffic in Ottawa; adjacent to a commuter highway in Ottawa and; regional background air in and around Windsor, Ontario), show that the different meteorological conditions and atmospheric processes result in different particle light absorption enhancement and hence the specific attenuation coefficient (SAC). Depending upon location of measurement and the BC spherule diameter (primary particle size – PPS) measurement from the LII, the SAC varies from 2.6±0.04 to 22.5±0.7 $m^2\,g^{-1}$. Observations from this study also show the active surface area of the BC aggregate, inferred from PPS, is an important parameter for inferring the degree of particle collapse of a BC particle. The predictability of the overall BC light absorption enhancement in the atmosphere depends not only on the coating mass but also on the source of the BC and on our ability to predict or measure the change in particle morphology as particles evolve.

1 Introduction

Black carbon (BC) particles are released into the atmosphere from incomplete combustion of fossil and biofuels, and biomass burning (Horvath, 1993). Based on different definitions and methods of detection, BC is sometimes referred to as "refractory carbon" or "elemental carbon", representing the solid carbon fraction in the particles with a high sublimation temperature, and is often quantified using thermal/optical methods

ACPD
10, 19939–19980, 2010

(Huntzicker et al., 1982; Turpin et al., 1990; Chow et al., 2001). When BC is measured based on light absorption spectroscopy techniques, such as an Aethalometer or a particle soot absorption photometer (PSAP), it is usually referred to as "light absorbing carbon" (Bond and Bergstrom, 2006; Bond et al., 1999). In some cases, BC is also commonly interchanged with other terms such as "soot" or "carbon black", while the true definition of BC is still subject to debate (Bond and Bergstrom, 2006). Regardless of the definition, combustion generated BC particles are not emitted as pure BC. Recent research of vehicular emission shows that the emitted particles often contain a mixture of substances, such as black carbon, volatile organic compounds, unburned fuel, unburned oil, sulphate, and metal ash (Burtscher, 2005; Kittelson, 1998; Park et al., 2003). In this work, BC particle is defined as the solid fraction of the combustion generated particle that absorbs a significant amount of radiation from a laser beam.

Atmospheric BC particles are an important global warming agent with radiative forcing similar in magnitude to carbon dioxide (Bond and Sun, 2005). BC alters the radiation budget of the Earth by absorbing incoming radiation from space or radiation emitted from the Earth's surface and then re-emitting it locally as heat energy thus warming the atmosphere. To accurately estimate and forecast the global warming effect due to BC knowledge on the light absorption properties of BC and an understanding how condensable materials that typically coat BC can affect the particle light absorption and thermal emission is required.

The effect on light absorption by atmospheric BC particles due to the presence of non-absorbing materials is complicated. A general increase in particle light absorption is observed with increased quantities of coating materials on the BC particles but the amount of absorption enhancement depends on factors such as refractive index of the coating materials, the size and location of the BC core, and also the wavelength of the light (Lack and Cappa, 2010; Bond and Bergstrom, 2006; Bond et al., 2006; Slowik et al., 2007a; Fuller et al., 1995; Shiraiwa et al., 2010; Dillner et al., 2001). At the same time particle light absorption decreases when the BC particle structure collapses from an aggregate or elongated form to a sphere-like particle (Fuller et al., 1999; Iskander

ACPD
10, 19939–19980, 2010

et al., 1991; Liousse et al., 1993) due to natural atmospheric processing, such as cloud processing and/or condensation of organic and inorganic materials onto BC particles (Ramachandran and Reist, 1995; Huang et al., 1994; Hallett et al., 1989; Johnson et al., 2005). The collapse of the BC structure was believed to be one explanation for the decreased particle light absorption observed at some ambient measurement locations (Lewis et al., 2009; Liousse et al., 1993; Liu et al., 2008; Chan et al., 2010). Although the BC morphology and coating issues may appear as independent phenomena, they are closely linked with respect to atmospheric BC particles.

A few studies were conducted in the past using laboratory generated BC particles coated with various materials in an attempt to understand the BC coating issue. Xue et al. (2009) coated BC particles generated from propane combustion with glutaric acid and succinic acid and then exposed the coated particles to a range of relative humidities. Using a differential mobility analyzer-aerosol particle mass analyzer (DMA-APM) system to measure the morphology of the BC particles, Xue et al. observed that the enhancement in the optical properties of BC due to coating material depended strongly on the ability of the coating to alter the morphology of the BC particles. Gangl et al. (2008) generated BC particles by spark discharge and coated the particles with the non-absorbing carnauba wax. An increase in absorption of up to a factor of 1.8 was observed. Coating graphite particles with oleic acid and glycerol, Shiraiwa et al. (2010) observed an enhancement in light absorption of 1.3 to 2 depending on the amount of coating present.

Although laboratory studies are useful, the challenge is to translate the results to the behaviour of BC when it is present and processed in the atmosphere. For this reason, some past studies have attempted to tackle the BC coating and morphology issue using ambient aerosols. The advantage of these kinds of studies is that the coating effect can be studied directly using aerosols present in the atmosphere and thus findings are expected to be more relevant to atmospheric applications. However, the measurements obtained in this work can be difficult to interpret due to the complexity of the ambient aerosols and changing atmospheric conditions. Knox et al. (2009) used

ACPD
10, 19939–19980, 2010

a thermodenuder to remove the particle coating on ambient particles that had different histories based on back trajectories analysis and then estimated their BC mass absorption cross-section (MAC). The MAC results for particles with and without the coating removed were not statistically different due to the large variations of the ambient measurements. Also, the authors suggested that the ambient particles present during the study were too large or heavily coated such that the amount of coating removed in the thermodenuder was insufficient for producing a measurable decrease in the absorption enhancement. Chan et al. (2010) observed that the specific attenuation coefficient (SAC) of ambient BC particles at a rural site was independent or decreasing with increasing particle coating mass or relative oxygenated organic mass. They suggested that the structural collapse of BC particles over time was one of the factors that led to a decrease in particle light absorption. The inconsistent observations between the laboratory and field measurements suggest that the atmospheric processing of BC particles and its relation to the light absorption is not well known.

With the objective to improve the understanding of the effect of coatings and morphology on fine BC particles, this study was conducted with ambient particles, using relatively fast time response instruments, a thermodenuder, and strategically selected measurement locations before, during and after an intensive field study, referred to as "The Border Air Quality and Meteorology Study" (BAQS-Met; Levy et al., 2010), which occurred in Southern Ontario, Canada, in the summer of 2007. There are two major components in this work. The first component is a thermodenuder experiment conducted at one location in the north part of the city of Toronto after the main BAQS-Met period. This was undertaken to characterize how two instruments, namely a Droplet Measurement Technologies (DMT) photoacoustic spectrometer (PA) and a high sensitivity laser-induced incandescence (LII) instrument, respond to ambient BC particles with different amounts of total particle coating mass, as measured by an Aerodyne quadrupole Aerosol Mass Spectrometer (AMS).

Concurrent measurements with the three instruments were obtained over several days with an alternating flow path – five minutes through the thermodenuder and five

ACPD
10, 19939–19980, 2010

minutes bypassing the thermodenuder. It was hypothesized that this unique combination of instrumentation would offer a valuable opportunity for studying BC particles. This is because of the different BC measurement principles for LII and PA. The former was expected to be less affected by coatings, thus only responding to BC by detecting the thermal emission produced by super-heated refractory fine carbon particles (e.g., Snelling et al., 2005; Moteki and Kondo, 2007). The light absorption (B_{abs}) measurements by PA were, however, observed to be sensitive to coatings (e.g., Knox et al., 2009). This is likely due to the lensing effect of the coatings and the lower laser power involved in producing the signal detected in the PA, which is derived from pressure waves produced by thermal heating of the boundary layer surrounding the particles. A possible secondary source of the pressure waves in the PA could arise from evaporation of coating materials on the particles. However, previous studies, which have mainly focused on the impact of water evaporation on the photoacoustic signal found that in most atmospheric applications the impact is generally small (Raspet et al., 2003; Raspet et al., 1999). Furthermore, Murphy (2009) found that any impact is reduced as the thickness of the organic coating increases. Thus, the coating evaporation impact was not investigated in this study and is assumed not to be the major factor affecting the variations in light absorption measured from the PA as a function of coating. While the lensing effect may increase the total absorption in LII measurements, the technique of Snelling et al. (2005) will automatically compensate for this, resulting in an unaffected measurement of BC volume and mass.

In the second component of our experiment, the instruments were deployed to contrasting locations to measure the ambient BC particles without thermaldenuder alterations. These measurements were undertaken to determine if it is possible to observe in situ urban to regional scale variations in the coating effect on BC light absorption properties within different air masses. It was expected that these data would provide new insights into how the particle light absorption varies across a realistic range of atmospheric conditions where there would be differences in the amount of particle coating mass and in particle morphology. Through the use of a mobile laboratory,

ACPD
10, 19939–19980, 2010

measurements were collected just before the main BAQS-Met study period in an urban street canyon with heavy diesel bus traffic and at a location adjacent to a highway, both of which were in Ottawa, Ontario. During BAQS-Met the mobile lab was deployed to an urban site in West Windsor, Ontario, and to rural locations in Southwestern Ontario. Through these strategic deployments our objective was to quantify the range of variability in the coating enhancement in BC light absorption in urban and near-urban situations and to test the hypothesis that atmospheric changes in particle morphology are an important additional factor to alter the BC light absorption enhancement caused by particle coating, particularly for fresh BC particles.

2 Sampling and instrumentation

2.1 Thermodenuder experiment

From 15–21 August 2007, ambient measurements were taken simultaneously by the three instruments at a suburban/commercial location located about 17 km north of downtown Toronto, Ontario. The main source of anthropogenic emissions in this area is from vehicles along a busy four lane road 150 m west of the measurement site. During morning and evening, rush hour traffic along this road is often "stop and go", but is dominated by gasoline vehicles, while during the day heavy and light duty diesel trucks also use this road frequently.

The instruments were housed inside a mobile laboratory, also known as the Canadian Regional and Urban Investigation System for Environment Research (CRUISER), which was connected to an external source of power. Ambient air was drawn into CRUISER and to the entrance of an automated sampling system at 16.7 L min^{-1} through a 3.18 cm OD stainless steel sampling tube of 1.88 m in length. Inside CRUISER this tube is surrounded by a 15.24 cm PVC pipe containing an external sheath air flow drawn from outside, which serves to keep the sample air containing particles at ambient temperature as long as possible to avoid condensation in summer

ACPD
10, 19939–19980, 2010

and evaporation in winter. This inlet, which is 3.6 m above ground (extending out of the roof of CRUISER) was equipped with a 2.5 micron sharp cut cyclone.

The automatic sampling system (Fig. 1) draws air from the base of the inlet system. Every five minutes the solenoid value changed position allowing the ambient sample to either pass through or bypass the thermodenuder (Dekati model ELA-111). When the ambient particles passed through the thermodenuder (~300 °C), a large fraction of the non-refractory components in the particles were evaporated and removed. The denuded or non-denuded samples were then drawn into the PA (1.0 L min^{-1}; 2 m of 0.64 cm O.D. mixed stainless steel and silicon conductive tubing) and LII (8.0 L min^{-1}; 4 m of 0.64 cm O.D. silicon conductive tubing) for measuring light absorption and inferred BC mass concentration and the AMS (83 cm^3 min^{-1}; 0.5 m of 0.64 cm O.D. silicon conductive tubing) for measuring the mass concentrations of the non-refractory components in the ambient particles including sulphate, nitrate, organic matter, and ammonium.

2.2 Ottawa highway and urban street canyon

The Ottawa measurements consist of a small data set that was acquired with CRUISER running on generator power at two different locations in Ottawa: 1) an area located near a local highway (near the intersection between HWY 417 and HWY 174) with sampling during the afternoon rush hour period and 2) a location in the Ottawa downtown area that is surrounded by tall buildings (Albert Street and Elgin Street) with sampling during the morning rush hour period when there is constant diesel bus traffic bringing commuters into the downtown core. The two locations were chosen to study how the PA and LII BC signals and their ratios change with different amounts of particle coating mass with the emitted particles having limited and some degree of atmospheric processing, at the street canyon and highway locations, respectively. No thermodenuder was used during the study as the goal was to observe changes in the light absorption properties induced by urban- to regional-scale atmospheric processes.

2.3 BAQS-Met field study

The BAQS-Met field study was part of the second component of this study, during which CRUISER was deployed to various locations inside and outside the city of Windsor. There are no major emission sources near the sampling locations. However, there were transported emissions from the Detroit-Windsor area and other regional emission sources to the sampling locations. When it was inside the city, CRUISER was parked the West Windsor Water Pollution Control Plant for several days for continuous measurements at which time it was connected to an external source of power. From time to time, CRUISER, running on generator power, was driven to different locations outside, but within approximately 50 km of the Detroit-Windsor area. CRUISER stopped for periods ranging from about 15 min to 1 h at locations expected to be experiencing different air masses affected by local lake-induced circulation patterns, which could potentially alter the extent of air mass processing within relatively short distances. During the BAQS-Met field study, the PA and LII were used to provide particle light absorption coefficient and inferred BC mass measurements while the AMS was used to measure the non-refractory component in the particles at the same time. The thermodenuder was not used during the BAQS-Met study as the goal was to observe changes in the light absorption properties induced by local to regional scale atmospheric processes.

2.4 Black carbon measurement

In this study, a Droplet Measurement Technology photoacoustic spectrometer (PA) and a high sensitivity laser-induced incandescence (LII), developed by the National Research Council Canada (NRC), were used for measuring BC in the ambient particles. The PA and LII are both in situ instruments capable of measuring BC in the particle directly from the airstream. PA does not measure BC mass directly but measures the particle light absorption coefficient (B_{abs}), which is proportional to the BC mass in the particles. LII measures the thermal emission, which is directly proportional to the BC mass. Therefore, PA and LII are close to being first principle instruments for measuring BC mass concentration (Moosmüller et al., 2008).

ACPD
10, 19939–19980, 2010

2.4.1 Photoacoustic spectrometer (PA)

In the PA, the laser beam (2 W, 781 nm) is modulated at a rate of 1500 Hz as it passes through the particle stream inside the PA resonator. This causes the surrounding air to expand and contract at the modulated frequency. The pressure disturbance (i.e., acoustic signal) is amplified within the photoacoustic resonator and then measured by a microphone. The acoustic signal is proportional to the black carbon mass concentration and reported as absorption coefficient (Arnott et al., 1999; Faxvog and Roessler, 1982; Lack et al., 2006). Dividing the absorption coefficient by the specific attenuation coefficient (SAC) gives an estimate of the BC mass concentration. The laser light scattered by the particles that are present inside the resonator is detected and measured by a photo multiplier tube (PMT) which is mounted on the middle sideway of the resonator. The signal is processed and reported as the particle light scattering coefficient (B_{scat}).

2.4.2 Laser-induced incandescence instrument (LII)

In the case for the LII, BC is heated by a high energy short pulse laser (200 mJ/pulse, 7 ns FWHM duration, 1064 nm wavelength). The laser energy is absorbed by the BC component in the particles causing a rapid increase in temperature. During the heating process, temperature of the BC component in the particle approaches ~4000 K, just below the sublimation temperature for BC. At these temperatures the particles incandesce (as a form of near-blackbody emission) with sufficient intensity to be detected. At the end of the laser pulse, heating ends and the BC particles cool rapidly, over a period of approximately one microsecond, at which point the incandescence signal is no longer detectable. The energy loss to the surrounding air is proportional to the active surface area of the BC particles. The NRC system is a high sensitivity variant of the auto-compensating LII (AC-LII) which employs two color pyrometry (at wavelengths of 445 nm and 750 nm) to determine the particle temperature from the incandescence signal (Smallwood, 2009). Based on the absolute magnitude of the incandescence signals combined with the BC particle temperature and the rate of heat

ACPD
10, 19939–19980, 2010

losses to the surrounding air, the BC concentration as well as the spherule diameter (primary particle size – PPS) can be determined, respectively (Mewes and Seitzman, 1997; Snelling et al., 1998, 2000, 2005; Wainner and Seitzman, 1999; Bryce et al., 2000; Schulz et al., 2006). The high sensitivity LII instrument has a BC measurement limit of 15 ng m^{-3} (Smallwood, 2009). The BC concentration is reported as a volume fraction (BC volume to air volume in the sample or soot volume fraction – SVF) and can be converted to a mass concentration through multiplying by the BC material density, 1.9±0.1 g cm^{-3} (Smallwood, 2009). Although the NRC AC-LII acquires data at a rate of 20-Hz, both the PA and LII were operated at 1-min time resolution during all measurements used in this study.

2.5 Aerosol mass spectrometer

During this study, the non-refractory components in the aerosol were measured by an Aerodyne quadruple Aerosol Mass Spectrometer (AMS). Inside the AMS, particles are drawn from ambient condition through an aerodynamic lens to focus into a narrow beam, accelerated to specific aerodynamic velocities that are related to the vacuum aerodynamic diameters of the particles. The particles impact on a resistively heated surface where all volatile and semi-volatile components are vaporized. Ionized by electron impact, fragments are then detected by a quadrupole mass spectrometer at about 10^{-7} Torr (Jayne et al., 2000; Jimenez et al., 2003; Allan et al., 2003). During this study, the AMS was operated in the mass and time of flight modes providing average mass concentrations of the organics, sulphate, nitrate, and ammonium in the particles. The time resolution used for the AMS during the thermodenuder experiment was 1 min. For the Ottawa field measurements the time resolution was 5 min. For the BAQS-Met measurements, the time resolution was 2 and 5 min when measurements were taken at various locations away from the city and 10 or 15 min when CRUISER was parked in the city. For all the AMS measurements, the collection efficiency (CE) was assumed to be unity. Discussion regarding the CE and its implication to the results are given in Sect. 3.2.

ACPD
10, 19939–19980, 2010

3 Data interpretation

3.1 Signal enhancement due to particle coating

The objective of the thermodenuder experiment was to determine the extent to which particle coatings influence the signals from the PA and LII instruments. The thermodenuder effectively removes semivolatile coatings thus maximizing the potential to detect and characterize the signal changes. The determination of the signal enhancement is illustrated in Fig. 2. Figure 2a shows a time series subset of the total particle coating mass, defined as the sum of organics matter, sulphate, nitrate, and ammonium mass concentration measured from the AMS. Every five minutes, particles passed through the thermodenuder causing a substantial decrease in particle coating mass in the range of 4–8 $\mu g\,m^{-3}$ (60–70%). In Fig. 2b, the red circle trace shows the B_{abs} measured by the PA during the same time period as in Fig. 2a. The example demonstrates that there is a change in the PA instrument response, interpreted as a change in the B_{abs}, when the thermodenuder removed mass (i.e., coating material) from the particles. In contrast, the SVF measured by the LII during the same period of time (Fig. 2c) shows no distinct changes between the denuded (black squares) and non-denuded (orange circles) conditions.

In addition, due to continual changes in the ambient conditions (e.g., heterogeneity in the aerosol due to different parcels of air being measured minute by minute) there are additional variations in B_{abs} beyond those imparted by the switching between denuded and non-denuded conditions. Thus, to calculate a representative signal enhancement (i.e., ΔB_{abs}), the median value during each five minute cycle was determined for the non-denuded and denuded (blue solid triangles and black solid diamonds in Fig. 2b) conditions, respectively. A cubic spline fit was then applied to these data points to estimate B_{abs} during the intervals when the sample was following the alternate flow path (non-denuded condition in blue open triangles and denuded condition in black open diamonds). This reduced the one-minute data to five-minute time resolution measurements. Finally, the difference in magnitude between the two B_{abs} baselines (indicated

ACPD
10, 19939–19980, 2010

by the black arrow) is assumed to be the best estimate of the signal enhancement during each time period. The signal enhancement determined from this method is built on three main assumptions: 1) the signal enhancement depends linearly on the total amount of the particle coating mass on the BC, 2) all subcomponents in the coating mass that are detected by the AMS and removed in the denuder (e.g., organics, sulphate, nitrate, etc.) contribute equally to the signal enhancement, and 3) particle loss due to diffusion and thermophoresis inside the thermodenuder are insignificant.

The choice of using the median value was made to minimize the impact caused by occasional fluctuations in the time-dependent data (as seen in Fig. 2b). Analyses (not included here) show that the value of B_{abs} estimated based on mean B_{abs} are on average 2% larger in magnitude than that determined using the median B_{abs} due to random fluctuations. In comparison, the coating enhancement ΔB_{abs} estimated using the average B_{abs} is 15% smaller than that obtained using the median B_{abs}.

The same analysis is also performed on the measurement signals from LII (i.e., SVF) to yield ΔSVF. As shown in Fig. 2c, the ΔSVF for the LII is significantly smaller than ΔB_{abs} from the PA and in many cases a ΔSVF is not observable. Discussion regarding the comparison in signal enhancements for the PA and LII is given in Sect. 4.2.1.

3.2 Total signal enhancement in an aerosol

In Sect. 3.1, ΔB_{abs} is determined by the difference in B_{abs} between the non-denuded and denuded conditions. This value will be the true coating enhancement provided that the thermodenuder removes the particle coating mass completely. Figure 3 shows the time series of the measured particle coating mass (black circles) for the non-denuded condition as determined by the AMS based on two assumptions. First, this measured mass is primarily contributed by the coating on a BC particle. Second, any liquid particles that are also sampled have the same average composition as the coating materials on the BC particles. Applying the technique described in Sect. 3.1 to the particle coating mass yields the amount of particle coating mass removed by the thermodenuder. The ratio of the two masses gives an estimate of the percentage of coating removed

ACPD
10, 19939–19980, 2010

each time the particle passes through the denuder; this is presented by the red trace in Fig. 3. During the course of the experiment, the thermodenuder removed close to or higher than 80% of the particle coating mass, but this varied among the 5 min samples due to variations in nature of the ambient particles. As the particle coating mass was not completely removed, the coating enhancement determined from Sect. 3.1 is only the apparent enhancement induced by the denuder removal. Thus, each 5 min measurement needs to be adjusted or normalized to the full effect of the coating before comparing across all data points in order to undercover more subtle reasons for changes in the magnitude of the coating enhancement. Based on our assumptions (Sect. 3.1), we can state that,

$$\frac{\Delta B_{\text{abs}}}{\Delta M_{\text{coating}}} = \frac{\delta B_{\text{abs}}}{\delta M_{\text{coating}}} \tag{1}$$

where ΔB_{abs} is the total signal enhancement caused by the total amount of particle coating mass $\Delta M_{\text{coating}}$ and δB_{abs} is a finite change in signal enhancement caused by a finite amount of particle coating mass δ_{coating} (i.e., the apparent changes measured by the thermodenuder experiment). Rearranging Eq. (1) gives the total signal enhancement in a particle as,

$$\Delta B_{\text{abs}} = \Delta M_{\text{coating}} \times \frac{\delta B_{\text{abs}}}{\delta M_{\text{coating}}} = M_{\text{bypass}} \times \frac{B_{\text{non-denuded}} - B_{\text{denuded}}}{M_{\text{non-denuded}} - M_{\text{denuded}}} \tag{2}$$

where $M_{\text{non-denuded}}$ and M_{denuded} are the particle coating mass measured during the non-denuded and denuded conditions, respectively. $B_{\text{non-denuded}}$ and B_{denuded} are the PA signal measured during the non-denuded and denuded conditions, respectively. This technique is equally valid to other quantities, such as dry SVF.

In this study, a value of unity was assumed for the AMS CE due to the lack of other supporting data for in situ estimation of the AMS CE. This however has no effect to the coating enhancement derived in Eq. (2). Using a unity AMS CE however does affect the normalized PA:LII ratio (i.e., PA:LII ratio divided by particle coating mass; see

ACPD
10, 19939–19980, 2010

Sect. 4.3.2). This implies that the normalized PA:LII ratios discussed in Sect. 4 of this work represent an upper limit of the particle light absorption enhancement.

4 Results and discussion

4.1 Air quality comparison among different sites

Table 1 summarizes the common parameters measured at the various sampling locations; these include the particle light absorption (B_{abs}) and scattering (B_{scat}) coefficients measured from the PA, the primary particle size (PPS) and soot volume fraction (SVF) determined from the LII, and the particle coating mass estimated from the AMS. Also included are the average breakdown percentages for the four major particle compositions (organics, sulphate, ammonium, and nitrate) for the different data sets. A parameter defined as the ratio of the particle light absorption to the soot volume fraction (PA:LII ratio) that is used as a surrogate to describe the B_{abs} signal enhancement (see Sect. 4.3) is included. The same quantity that is normalized by the total particle coating mass is also included. Table 1 also includes the calculated specific attenuation coefficient (SAC; calculated by Eq. (3) in Sect. 4.5) for various sites. All values in bold represent the mean value. Standard deviation and the total number of valid data points are given in brackets. Finally, the data resolution indicates the AMS resolution which the PA and LII data were averaged to.

The highest BC concentrations, as inferred from B_{abs} and SVF were observed in the Ottawa street canyon. The location with the next highest levels was by the highway in Ottawa. Interestingly, B_{abs} was higher at the Toronto suburban site compared to the Windsor area, while the opposite pattern was observed for SVF. This may be related to the smaller PPS of the BC particles at Toronto, as will be discussed below. The light scattering and signal enhancement generally, but not always followed the same site to site pattern as the particle coating mass. The most obvious case is the B_{scat} values for the Windsor data which are small despite of the largest amount of particle coating mass

ACPD
10, 19939–19980, 2010

present on the particles. The particles observed at Windsor are aged and more likely approached a spherical-like structure. Since we do not have evidence to show that the measurements at Windsor were erroneous, we speculate that the B_{scat} obtained from other sites may have been enhanced due to the non-spherical nature of the particles. As will be discussed in the next few sections, the particle morphology plays an equal or potentially more important role in these cases in affecting the signal enhancement.

As expected, the measurement locations and time periods included in this study experienced different meteorological conditions and atmospheric processes. This is reflected by the coating mass as well as the percentage of sulphate to the coating mass. The particles observed at Toronto are believed to be the least aged based on the observed PPS values and the least amount of coating mass. Over time, more organic material and sulphate are condensed on the particles causing the relative organic matter mass percentage to increase, followed by a slower increase in sulphate to total coating mass. Therefore, for the measurement periods reported here, the particles observed at and around Windsor, which has the highest sulphate mass percentage compared to other sites as well as the largest amount of coating materials, are believed to be the most aged.

4.2 Thermodenuder experiment

4.2.1 Signal enhancements due to particle coating mass

Figure 4a shows the variations in the total signal enhancement in particle light absorption (ΔB_{abs}) measured by the PA as a function of the particle coating mass. The ΔB_{abs} has been corrected using Eq. (2) to represent enhancement due to the total amount of the coating mass present on a particle. Each individual box represents the 25th, 50th, and 75th percentiles of the measurement values while the 10th and 90th percentiles are represented by the bottom and top whiskers, respectively. The total number of data points for each category is given in the lower bottom axis. These results demonstrate that there is an observable signal enhancement in particle B_{abs} measured by the PA

ACPD
10, 19939–19980, 2010

and the magnitude of the enhancement is considerably larger when the particle coating mass is large.

During periods when particles contain a small amount of coating materials the B_{abs} for denuded and non-denuded conditions are similar in magnitude (small ΔB_{abs} values). In such situations fluctuations in BC concentration among 5 min periods becomes the main source of variation in ΔB_{abs} and can cause occasional negative enhancements. Region I in Fig. 4a, for particle coating masses of 0–5 $\mu g\,m^{-3}$, where ΔB_{abs} increases with increasing coating mass, can be fitted adequately by a linear regression line which gives a slope of $0.35\pm0.07\,(M\,m)^{-1}\,(\mu g\,m^{-3})^{-1}$. One of the more striking patterns in the figure is that the signal enhancement does not increase through the entire range of particle coating mass, but appears to plateau before dropping to lower values. Within the plateau region (i.e., region II, for particle coating masses of 5–11 $\mu g\,m^{-3}$), particle coating on average consisted of 70–88% organic matter, while sulphate, ammonium, and nitrate contributed 4–15%, 5–12%, and 2–4%, respectively (Fig. 4d). These results show that when the coating has accumulated to certain mass range, about 5 to 11 $\mu g\,m^{-3}$ in this case, the absorption enhancement becomes relatively steady despite the change in coating quantity or composition. Applying a linear regression fit to the ΔB_{abs} over this region gives a regression slope of $0.01\pm0.09\,(M\,m)^{-1}\,(\mu g\,m^{-3})^{-1}$, implying that the absorption enhancement remains constant during this stage. The plateau region suggests that when the particle coating has grown to considerable size the relationship between the coating enhancement and the amount of coating mass becomes weak. As a result, much larger increases in particle coating mass are required to cause further increases in absorption, as predicted by Bond et al. (2006).

In areas where fresh emissions are contributing to the BC continual accumulation of coating materials can cause a collapse of the BC aggregate. In this case the enhancement caused by the aggregate structure disappears, which leads to a decrease in the overall ΔB_{abs}. Such a behaviour is seen in Fig. 4a where there is a decrease in ΔB_{abs} in the transition between regions II and III. We hypothesize that through nat-

ACPD
10, 19939–19980, 2010

ural atmospheric processes BC aggregates collapse, leading to an abrupt change in apparent BC absorption, as observed in Fig. 4a. Indeed previous field and laboratory observations have shown that condensed water (Ramachandran and Reist, 1995; Huang et al., 1994), sulfuric acid (Pagels et al., 2009), and other organic materials (Slowik et al., 2007b) can all lead to collapse of BC aggregate. However, the amount of coating mass required to induce this change was not reported. Results from this study suggest that a lower limit estimate of this threshold at suburban Toronto is about $10\,\mu g\,m^{-3}$. However, the exact value may vary depending on the BC source and on a variety of atmospheric processes, although further research is needed to understand these factors and the time scales involved.

The small ΔB_{abs} values at a high particle coating mass indicate that there is no absorption enhancement for the denuded and non-denuded samples. Interestingly, this result is consistent with the observations from Knox et al. (2009) who observed no statistical differences in absorption enhancement for particles present in aged air masses with and without the coating removed.

Figure 4b shows the variations of the signal enhancement in particle light scattering (ΔB_{scat}) measured by the PA as a function of the particle coating mass. Unlike ΔB_{abs}, ΔB_{scat} increases throughout the full range of particle coating mass and also increases more rapidly. The ΔB_{scat} measurements on Fig. 4b can be fitted well with a power function; this indicates that the light scattering, as might be expected, is influenced more-dramatically by the amount of particle coating materials.

In comparison to the PA observations, regardless of the amount of coating mass on the particles, there is no signal enhancement in the SVF (ΔSVF) measured by the LII (Fig. 4c). Applying a linear regression fit to the measurements in Fig. 4c gives a slope of $(8.36\pm0.44)\times10^{-17}\,(\mu g\,m^{-3})^{-1}$. Applying the material BC density of $1.9\,g\,cm^{-3}$ to the regression slope shows that LII gives $(0.16\pm0.01)\,ng\,m^{-3}$ of apparent BC mass concentration for every $1\,\mu g\,m^{-3}$ of coating mass present on a particle. The regression slope in Fig. 4c also suggests that the increase in the apparent BC mass concentration is insignificant compared to detection limit of the instrument (i.e., y-intercept). Based

ACPD
10, 19939–19980, 2010

on the regression analysis, the estimated detection limit is 14.76±6.08 ng m^{-3}. This is consistent with the 15 ng m^{-3} measurement limit for the high sensitivity LII (Smallwood, 2009).

Returning to the PA ΔB_{abs} measurements in regions I and III, the best fit slopes are 0.35 (M m)$^{-1}$ (µg m^{-3})$^{-1}$ and 0.28 (M m)$^{-1}$ (µg m^{-3})$^{-1}$, respectively. Applying the observable range of SAC values from this study (2.6 to 22.5 m^2 g^{-1} based on Eq. (3); Table 1) to these regression slopes gives a range for the apparent BC mass concentration of from 0.01±0.01 µg m^{-3} to 0.13±0.03 µg m^{-3} per every 1 µg m^{-3} of coating mass present on a particle, respectively.

The contrasting results between the coating impact on PA and LII determination of BC mass, which were expected, are related to substantial differences in the measurement principles between the PA and LII. In the case of LII, the absorbed laser energy is sufficient to heat the BC to temperatures that will evaporate any volatile or non-refractory substances on the particle, eliminating their role in the transfer of the laser energy to the BC in the particle and hence in the absolute measurement of BC. Secondly, the AC-LII approach (Snelling, 2005) compensates for any reduction in particle temperature due to the evaporation of volatiles. Thus, as hypothesized, the amount of particle coating does not influence the LII measurements of SVF. This result is consistent with observations from other studies using laser-induced incandescence based instruments such as the Single Particle Soot Photometer (e.g., Slowik et al., 2007a).

In the case of the PA, much less, if any evaporation occurs due to the lower energy of the laser, which has limited impact on particle temperature. Consequently, the presence of particle coating contributes to a lensing effect by concentrating the PA laser energy into the BC core thus enhancing absorption, similar to what is predicted to occur when atmospheric particles interact with the sun's energy (Bond et al., 2006).

The thermodenuder results suggest that parallel measurements of atmospheric BC with LII and PA can provide in situ, fast time-response information on the enhancement in light absorption due to particle coating. However, as will be discussed next, particle size or morphology appears to be another important dimension influencing the

ACPD
10, 19939–19980, 2010

relationship between BC amount and light absorption for freshly emitted BC particles.

4.3 Factors affecting particle light absorption

4.3.1 BC particle morphology and spherule diameter

BC particles are formed during combustion at temperatures between about 1000 and 2800 K, at pressure of 50 to 100 atm inside both gasoline and diesel powered engines, but primarily from the latter (Heywood, 1988). The BC formation and oxidation processes are completed before the exhaust exits the combustion engine. The BC formation process can be summarized by a series of steps with an initial nucleation process to produce the BC precursors, followed by a vapour to particle surface growth process to form the BC spherules up to about 10 to 20 nm, and then by the agglomeration process, which leads to the formation of the chainlike or aggregate structures (Amann and Siegla, 1982; Heywood, 1988). Diesel particulate matter collected at a conventional dilution tunnel may also contain 10–30% unburned hydrocarbons by mass (Amann and Siegla, 1982).

Particle morphology is known to play a role in affecting particle light absorption (Fuller et al., 1999) and this effect was investigated in this study through the use of the primary particle size (PPS) measured by the LII. Theoretically, the PPS refers to the diameter of the individual spherule that makes up BC particle chains or aggregates. In the LII the PPS is estimated or inferred by measuring the rate of heat loss of the particle to the surrounding air and then comparing this to calculations for estimating the available active surface area per unit volume air for heat transfer; this can then be related to the size of the spherules assuming the spherules within an aggregate are in point contact with each other. Observations show that freshly emitted BC particles measured from diesel exhaust usually have low PPS values ranging from 10 nm to about 30 nm (Smallwood, 2009). Over time, emitted particles undergo atmospheric processes and pick up condensable materials such as organic materials and sulphate (e.g., Johnson et al., 2005) and during cloud processing water molecules continue to condense and

ACPD
10, 19939–19980, 2010

evaporate from the BC particles (e.g., Ramachandran and Reist, 1995; Huang et al., 1994; Hallett et al., 1989). During such processes, the different amounts and types of materials present on the BC aggregate may induce a change in surface tension of the BC particle causing the structure to collapse. As the BC aggregate collapses, some of the surface area becomes shielded and is not available for heat transfer and this leads to an increased PPS value as inferred from LII (Smallwood, 2009).

Given that the PPS determined from LII is also a measure of the particle collapse, in this study an increasing trend of the PPS value is also assumed to be a surrogate for particle collapse. However, due to the complexity of the aggregate structure, the degree of collapse may not be a continuous variable but a categorical variable with complex behaviour. Nonetheless, this assumption is expected to be reasonable for combustion generated BC particles (e.g., diesel aggregates), particularly during the earlier part of their life in the atmosphere when they start as more branched structures allowing LII to detect the actual and smaller PPS. Conversely, in situations when the original aggregate is less branched or partially collapsed, it is likely that PPS will be less variable over time and the lower and upper limit of the PPS will appear to be more constrained. It is worth noting that the PPS value inferred from LII does not directly measure the structure of the BC particles. It is possible for particles to have different structures but still be made up by spherules with the same diameter, which may or may not impact the PPS inferred by LII. Other combinations of true spherule size and structure could also have similar PPS values. The uncertainty imparted by this variability likely results in it being more difficult to infer physical patterns when comparing PPS among widely separated time periods or measurement locations.

4.3.2 Measuring the light absorption enhancement

As the SVF from the LII measurement is independent of the particle coating mass while the PA B_{abs} measurement is not (Fig. 4a and c), we propose that the ratio of PA signal to LII signal (denoted as PA:LII ratio) can be used as an in situ measure of signal enhancement due to coating. Thus, the impact of the coating on the particles measured in

ACPD
10, 19939–19980, 2010

a given time interval can be determined without needing to perturb conditions through use of a thermodenuder, which will give more representative measurements of the impact of coating on light absorption. Furthermore, since these measurements can be taken with 1 min time resolution and both are responding to the variation in the signal that is caused by real variation in the ambient BC concentrations, it is possible to quickly compare different atmospheric particles types or air masses in terms of how the coating enhancement varies.

For ambient measurements, the light absorption enhancement observed from the PA:LII ratio consists of enhancements impacted by particle morphology, amount of coating materials and possibly by BC mass concentration. To properly compare the measurements, the PA:LII ratio proposed above is normalized by the particle coating mass estimated from the AMS. The normalized PA:LII ratio can be viewed as the light absorption enhancement per unit mass concentration of coating materials as it removes the additional enhancement caused by varying amount of the coating mass on the particles. This allows various measurements obtained at different times and locations to be combined to study the morphology enhancement of BC nanoparticles.

4.4 Signal enhancement from ambient measurements

Figure 5a shows the normalized PA:LII ratio as a function of PPS measured at Toronto, Ottawa (street canyon and near highway), and Windsor. The corresponding measurements are summarized in Table S1, S2, S3, and S4 in the Supplement, respectively. Measurements from all field studies are first separated according to different ranges of BC mass concentration (calculated from the SVF as it is independent of the coating mass). The data are then grouped according to the various ranges of PPS. As the normalized PA:LII ratio has removed the enhancement caused by various amount of coating mass, data in Fig. 5 represent the best estimate of the enhancement caused by the morphology of the ambient BC particles, which is likely to relate to the age of the BC particles. Combining measurements across all sites, a generally consistent pattern is revealed: The highest normalized PA:LII ratio occurs at the lowest PPS. The

ACPD
10, 19939–19980, 2010

normalized PA:LII ratio decreases with increasing PPS up to about 70 nm and then increases gradually for larger PPS values.

The Toronto measurements exhibit the highest enhancement compared to other data sets. The BC particles observed in Toronto also had the smallest PPS values suggesting that most of these particles are freshly emitted and are likely to be in an aggregate form. There are two points, labelled as A and B in Fig. 5a, that are outliers in the decreasing trend in normalized PA:LII ratio with increasing PPS (below 70 nm). The average particle composition for most measurement points in Fig. 5 are close to the grand average values. However, for points A and B, the organics to sulphate ratios are 7 and 15, respectively, which are higher than the average ratio of 5 using the grand average composition values. Also, point A and B represent an average value of eight and three 5-min continuous measurements, respectively. In comparison, these are relatively short periods compared to other data points in the Toronto data set. For example, data points with BC mass concentration between 0.02 to 0.11 $\mu g\,m^{-3}$ (orange triangle) with PPS less than 30 nm are averages of 43 and 30 data points, respectively. Data points with BC mass concentration between 0.11 and 0.20 $\mu g\,m^{-3}$ (green diamond) are averages of 10 to 19 data points. Therefore, these might imply that points A and B represent a brief moment with a different air mass containing BC particles with a different structure than most that were observed in Toronto. As a result, points A and B seem to have a different trend compared to the rest of the measurements.

Excluding points A and B, the Toronto data exhibit a decreasing trend towards larger PPS values with a reasonable continuity with the Windsor and Ottawa measurements. If the inferred primary spherule diameter from the LII (i.e., PPS) can be used to infer the degree of particle collapse, particles with very small PPS correspond to highly branched, with complex structure, fresh BC aggregates. As the BC aggregate is more effective than a spherical BC particle in enhancing light absorption (Fuller et al., 1999), this is the reason why particles with 10 to 50 nm PPS have larger enhancement than those in the 50 to 70 nm range. The relatively large variability in the Toronto data set about the trend is due to the highly variable/non-uniform and complex structure

ACPD
10, 19939–19980, 2010

(elongated vs. branched) of fresh BC aggregates due to the wide range of engine and operating conditions within the vehicle fleets on the roads in or upwind of the areas of our measurements.

During the BAQS-Met field study, CRUISER was parked inside the city of Windsor for several days of near-continuous measurements and then deployed to several locations away from the city for short term measurements. The small set of measurements that were taken outside of the city of Windsor are not statistically different from those taken within the city and therefore the two sets of measurements are combined and presented together in this section. Data obtained at and around Windsor show the lowest enhancement among all other data sets. The enhancement values for various BC mass concentrations are similar and the trend in the normalized PA:LII ratio across the entire range of PPS values is gradual. The ratio decreases with increasing value of PPS to about 70 nm and then gradually increases for larger PPS. The data suggest that most of the BC particles observed in the Windsor area were not fresh and were likely already collapsed to a large extent. However, further compacting of the BC structure and accumulation of condensable materials onto the particle led to a continued and observable increase in the PPS and a slow increase in B_{abs} enhancement per unit coating mass, respectively.

When sampling in the Ottawa street canyon, the tall buildings helped confine the vehicle emissions (especially from the diesel buses). This is reflected by the higher BC concentrations (Table 1). In contrast, sampling near the Ottawa highway in the afternoon (more vertical mixing) and with no large barriers to particle transport in and out of the area enhanced dilution of the BC particles leading to lower ambient BC concentrations (Table 1). When compared to the Toronto and Windsor data sets, the BC particles observed in Ottawa had intermediate PPS values ranging from about 40 nm to 80 nm, which is larger than those observed in Toronto. Coagulation is one possible reason for enhancing the collapse of the particle. This would explain the relatively larger PPS values for the particles measured in Ottawa. The Ottawa street canyon measurements generally show higher normalized PA:LII values compared to those from the Ottawa

ACPD
10, 19939–19980, 2010

near highway measurements. This is likely due to the fact that the street canyon measurements were strongly impacted by diesel powered buses while the near highway site was dominated by gasoline powered vehicles. We speculate that the diesel BC particles observed in the street canyon (particularly at high BC concentrations) were still in a more open aggregate form while the gasoline BC particles were more collapsed (see Section 4.5); this leads to a relatively higher B_{abs} enhancement in the diesel BC particle dominated street canyon data set.

4.5 Variations of the SAC with particle morphology

In situations when the light absorption from a BC particle is enhanced due to factors such as coating a higher value would be inferred for the SAC. Conversely, if a known amount of BC mass ages and relative quantities of other light absorbing species (e.g., brown carbon) increase, then its B_{abs} will be larger for the same amount of BC mass without coating, but less than the situation when the coating is composed of pure light scattering (non-absorbing) materials (Lack and Cappa, 2010). Under these circumstances the SAC derived from a more aged sample would be smaller.

The concurrent PA and LII measurements in this study were sampling the same air and thus equating their two definitions of BC mass concentration yields the SAC:

$$\mathrm{SAC}(\mathrm{m^2\,g^{-1}}) = \frac{B_{abs}}{\mathrm{SVF} \times \rho_{soot}} \quad (3)$$

Figure 6a shows the variation in the calculated SAC for all data. These results are also summarized in Tables S5 to S8 in the Supplement. As in Fig. 5, the data in Fig. 6 are first separated according to different BC mass concentration ranges and then grouped according to different PPS ranges. The grand average value of the SAC at the Toronto location, the Ottawa street canyon, the Ottawa near highway, and in and around Windsor are 22.5±0.7 $\mathrm{m^2\,g^{-1}}$, 11.2±1.0 $\mathrm{m^2\,g^{-1}}$, 6.5±0.8 $\mathrm{m^2\,g^{-1}}$, and 2.6±0.04 $\mathrm{m^2\,g^{-1}}$, respectively (Table 1). These results are generally within the range of values reported elsewhere (Liousse et al., 1993; Martins et al., 1998; Sharma et al., 2002; Snyder and

ACPD
10, 19939–19980, 2010

Schauer, 2007; Chan et al., 2010), providing some confidence in the use of SVF from the LII for estimating the BC mass concentration.

Generally, the SAC values in Fig. 6a can be divided into three main sections. For particles with PPS<40 nm the SAC values are large, in the range of 20–30 $m^2\,g^{-1}$; this is similar to measurements that were obtained in Congo, Ivory Coast (20 $m^2\,g^{-1}$; Liousse et al., 1993) and the winter and summer measurements at Alert, Canada (19–28 $m^2\,g^{-1}$; Sharma et al., 2002). In Fig. 6a, when PPS>70 nm the SAC values are small, in the range of 2–4 $m^2\,g^{-1}$. These value are consistent with US urban summertime measurements at the University of Rochester (2.7 $m^2\,g^{-1}$) and in downtown Philadelphia (3.3 $m^2\,g^{-1}$; Jeong et al., 2004), with late spring measurements at the rural site of Egbert in Central Ontario, Canada (3.8 $m^2\,g^{-1}$; Chan et al., 2010), and with measurements at the remote site of Mace Head Ireland (5 $m^2\,g^{-1}$; Liousse et al., 1993). In between 40 nm and 70 nm the SAC values are highly variable covering the range of values seen for the small and large PPS values, especially for PPS from 40–50 nm. Possible reasons for this behaviour are discussed in the following paragraphs.

When the PPS is less than 40 nm the BC particles are fresh and in chainlike or aggregate forms. Both of these morphologies tend to cause a larger particle B_{abs} value for a given BC mass and lead to a larger SAC, as shown in Fig. 6. Most of the Toronto data are in this section of the plot, with the largest SAC values despite relatively low BC concentrations. This is because although the BC mass is low the B_{abs} is relatively large due to the enhancement caused by the complex morphology associated with fresh emissions which more efficiently absorbs light and is more-impacted by coatings.

When the PPS is larger than 70 nm BC particles are aged, regardless of the source, and therefore the BC particles tend to be fully collapsed and more spherical in shape. Consequently, the B_{abs} enhancement is smaller and the resulting SAC values are the smallest among the suite of measurements. Particles with a PPS>70 nm may continue to experience growth in coatings, but this has a small and gradual effect on SAC due to the larger sizes of the particles. The particles observed in and around Windsor were the most aged and, not surprisingly, were mainly within this section of Fig. 6.

ACPD
10, 19939–19980, 2010

The wide range of observed SAC values in the middle section of Fig. 6a indicates that when the PPS is between 40 and 70 nm the situation is more complicated. We hypothesize that the cause of this observation is that unlike when PPS is <40 nm or >70 nm there are large differences in the origin and history of the particles associated with a 40–70 nm PPS. This leads to a range of SAC values among the measurements shown in Fig. 6a. For example, fresh diesel emissions could produce particles with a variety of PPS values within the 40–70 nm range depending upon the processes involved. The smaller end of this range would reflect particles consisting of chainlike aggregates with a minimal amount of collapse, which likely represents the typical situation with relatively large SAC values. In contrast, larger PPS values could arise in fresh diesel emissions during situations with frequent acceleration. In a situation like the Ottawa street canyon, where all the buses were constantly accelerating after stopping to let off passengers or near the Toronto site, where "stop and go" traffic is common, large numbers of BC particles would be generated within a short period of time and within a small area. This high number density would result in a greater potential for coagulation to form slightly collapsed and larger aggregates (i.e., increases the PPS value). In the street canyon or during rush hour there is also the potential for particles to remain nearby for longer periods so that less fresh diesel particles are observed to occur relatively close to the traffic. Due to natural processes (i.e., aging) the aggregates of these particles would also tend to be partially collapsed. Thus, in the vicinity of diesel traffic there can be a range of PPS values. At the same time the amount of coating can vary, although diesel BC particles tend to contain less coating material due to the relatively lean running conditions (Heywood, 1988). Thus, the resulting SAC values would be relatively small such as the Toronto points in Fig. 6 with SAC values around 15 $m^2\,g^{-1}$ or the even smaller SAC values for some of the points shown for the street canyon.

Another cause of the points in Fig. 6a with small SAC values within the 40–70 nm PPS range is gasoline engine emissions. These particles would need to have a relatively small B_{abs} for a relatively large SVF. In gasoline powered engines the fuel/air ratio usually varies from 0.8 to 1.2 and the combustion efficiency may vary from 95 to

ACPD
10, 19939–19980, 2010

80% (Heywood, 1988). This would lead to a high pre-catalyst hydrocarbon concentration. We hypothesize that these unburned hydrocarbons would reach super-saturation and condense on the BC particles after exiting the engine, but before the catalyst, when the temperature and pressure are both dramatically reduced. These combustion and exhaust conditions would cause the generally smaller BC particles associated with gasoline combustion to collapse, increasing the PPS and decreasing the B_{abs} enhancement before exiting the tailpipe. These BC particles would tend to result in smaller SAC values. The authors are not aware of any direct measurements to prove such a hypothesis, but a previous laboratory study provides support for this hypothesis. Using propane/O_2 flame to generate BC particles, Slowik et al. (2004) showed that BC particles remain as fractal aggregate when the fuel equivalence ratio (actual fuel oxygen ratio to stoichmetric fuel oxygen ratio) is low and become spherical in shape when the fuel equivalence ratio is much higher.

4.6 Atmospheric implications from this study

The results from this study demonstrate that particle coating has a positive impact on the light absorption of BC particles confirming results from laboratory studies. For freshly emitted BC particles, the morphology enhancement is important and should not be ignored. The morphology enhancement quickly diminishes as the BC particle structure collapses, which can be induced by many atmospheric processes, such as cloud processing and condensation of organic and/or inorganic materials onto BC particles. As that happens, it reduces the SAC and the atmospheric lifetime of the BC particles, by enhancing its removal through wet and dry deposition. The time required for the BC aggregate to collapse depends on the availability and extent of the atmospheric processes, which likely varies temporally (e.g., seasonally) and geographically. Therefore particle morphology is an important factor to consider when estimating BC particle light absorption and lifetime in the atmosphere once emitted from various combustion processes. Applying the total amount of condensable material on a particle to the results in Fig. 5 and 6 gives an upper limit estimation of the BC absorption enhancement and specific attenuation coefficient for atmospheric particles, respectively.

ACPD
10, 19939–19980, 2010

5 Conclusions

A thermodenuder was used at an urban site to study the effect of volatile and semi-volatile particle coating mass on fine BC particles using the photoacoustic spectrometer (PA) and laser-induced incandescence (LII) instruments. Results show that the black carbon (BC) measurements obtained from LII are independent of the particle coating mass. The BC mass concentration measured through the PA can be enhanced by the presence of the volatile and semi-volatile particle coating. As expected the aerosol light scattering can be predicted by the total amount of volatile and semi-volatile particle coating mass on the particle, however, the same can not be said for particle light absorption unless the particle morphology remains constant during the period for acquiring the volatile and semi-volatile particle coating. Ambient measurements at four different locations show that the specific attenuation coefficient (SAC) vary from $22.5 \pm 0.7\,m^2\,g^{-1}$ for freshly emitted BC aggregates to $2.6 \pm 0.04\,m^2\,g^{-1}$ for mostly collapsed BC particles (Table 1). These variations are closely related to the different BC sources (e.g., different types of engines and/or operating conditions) and the meteorological conditions which affect the type and amount of atmospheric processing. Overall, combining data from four different locations reveals that the value of the SAC is generally large when the primary particle size (PPS) is small (i.e., freshly emitted BC) while for a larger PPS (i.e., aged BC) the SAC values are small. In the intermediate PPS range, where a wide range of emission and atmospheric processes results in the characteristics of the particles varying significantly, prediction of the particle SAC requires a detailed understanding of the particle history. This study shows that a parallel PA and LII system is a useful technique for measuring BC light absorption enhancement and the results provide new insights and new estimates of the upper limit of this enhancement and the specific attenuation coefficient given that the amount of particle coating mass and the spherical diameter of the BC particles were known.

ACPD
10, 19939–19980, 2010

Supplementary material related to this article is available online at: http://www.atmos-chem-phys-discuss.net/10/19939/2010/acpd-10-19939-2010-supplement.pdf.

Acknowledgements. The authors sincerely thank Julie Narayan and Cris Mihele for their assistance in collecting, organizing, and providing the CRUISER measurements used in this study. The authors also want to thank Peter Barton and Jacek Rostkowski for their useful discussions regarding the characteristics and operations of the gasoline and diesel powered engines. This research was supported in part by PERD Particles and Related Emission Project C11.008, PERD AFTER Project C23.006, and CCTII Project TIB6.15, which are programs administered by Natural Resources Canada. Some funding for Tak W. Chan came from Environment Canada through Natural Sciences and Engineering Research Council (NSERC) postdoctoral visiting fellowship.

References

Allan, J. D., Jimenez, J. L., Williams, P. I., Alfarra, M. R., Bower, K. N., Jayne, J. T., Coe, H., and Worsnop, D. R.: Quantitative sampling using an Aerodyne aerosol mass spectrometer, 1, Techniques of data interpretation and error analysis, J. Geophys. Res., 108(D3), 4090, doi:10.1029/2002JD002358, 2003.

Amann, C. A. and Siegla, D. C.: Diesel particulates – what they are and why, Aerosol Sci. Tech., 1, 73–101, 1982.

Arnott, W. P., Moosmüller, H., and Rogers, C. F.: Photoacoustic spectrometer for measuring light absorption by aerosol: instrument description, Atmos. Environ., 33, 2845–2852, 1999.

Bond, T. C., Anderson, T. L., and Campbell, D.: Calibration and intercomparison of filter based measurements of visible light absorption by aerosols, Aerosol Sci. Tech., 30, 582–600, 1999.

Bond, T. C. and Sun, H.: Can reducing black carbon emissions counteract global warming?, Environ. Sci. Technol., 39, 5921–5926, 2005.

Bond, T. C. and Bergstrom, R. W.: Light absorption by carbonaceous particles: an investigative review, Aerosol Sci. Tech., 40, 27–67, 2006.

Bond, T. C., Habib, G., and Bergstrom, R. W.: Limitations in the enhancement of visible light

ACPD

10, 19939–19980, 2010

absorption due to mixing state, J. Geophys. Res., 111, D20211, doi:10.1029/2006JD007315, 2006.
Bryce, D. J., Ladommatos, N., and Zhao, H.: Quantitative investigation of soot distribution by laser-induced incandescence, Appl. Optics, 39, 5012–5022, 2000.
Burtscher, H.: Physical characterization of particulate emissions from diesel engines: a review, J. Aerosol Sci., 36, 896–932, 2005.
Chan, T. W., Huang, L., Leaitch, W. R., Sharma, S., Brook, J. R., Slowik, J. G., Abbatt, J. P. D., Brickell, P. C., Liggio, J., Li, S.-M., and Moosmüller, H.: Observations of OM/OC and specific attenuation coefficients (SAC) in ambient fine PM at a rural site in central Ontario, Canada, Atmos. Chem. Phys., 10, 2393–2411, doi:10.5194/acp-10-2393-2010, 2010.
Chow, J. C., Watson, J. G., Crow, D., Lowenthal, D. H., and Merrifield, T.: Comparison of IMPROVE and NIOSH carbon measurements, Aerosol Sci. Tech., 34, 23–34, 2001.
Dillner, A. M., Stein, C., Larson, S. M., and Hitzenberger, R.: Measuring the mass extinction efficiency of elemental carbon in rural aerosol, Aerosol Sci. Tech., 35, 1009–1021, 2001.
Faxvog, F. R. and Roessler, D. M.: Mass concentration of diesel particle emissions from photoacoustic and opacity measurements, Aerosol Sci. Tech., 1, 225–234, 1982.
Fuller, K. A., Malm, W. C., and Kreidenweis, S. M.: Effects of mixing on extinction by carbonaceous particles, J. Geophys. Res., 104, 15941–15954, 1999.
Gangl, M., Kocifaj, M., Videen, G., and Horvath, H.: Light absorption by coated nano-sized carbonaceous particles, Atmos. Environ., 42, 2571–2581, 2008.
Hallett, J., Hudson, J. G., and Rogers, C. F.: Characterization of combustion aerosols for haze and cloud formation, Aerosol Sci. Tech., 10, 70–83, 1989.
Heywood, J. B.: Pollutant formation and control in internal combustion engine fundamental, Ch. 11, in: Internal combustion engine fundamental, edited by: Duffy, A. and Morriss, J. M., McGraw-Hill, Inc., New York, 567–660, 1988.
Horvath, H.: Atmospheric light absorption – a review, Atmos. Environ., 27A, 293–317, 1993.
Huang, P. F., Turpin, B. J., Pipho, M. J., Kittelson, D. B., and McMurry, P. H.: Effects of water condensation and evaporation on diesel chain-agglomerate morphology, J. Aerosol Sci., 25, 447–459, 1994.
Huntzicker, J. J., Johnson, R. L., Shah, J. J., and Cary, R. A.: Analysis of organic and elemental carbon in ambient aerosols by a thermal-optical method, in: Particulate Carbon – Atmospheric Life Cycle, edited by: Wolff, G. T. and Klimisch, R. L., Plenum Press, New York, 79–88, 1982.

ACPD
10, 19939–19980, 2010

Iskander, M. F., Chen, H. Y., and Penner, J. E.: Resonance optical absorption by fractal agglomerates of smoke aerosols, Atmos. Environ., 25A, 2563–2569, 1991.
Jayne, J. T., Leard, D. C., Zhang, X., Davidovits, P., Smith, K. A., Kolb, C. E., and Worsnop, D. R.: Development of an aerosol mass spectrometer for size and composition analysis of submicron particles, Aerosol Sci. Tech., 33, 49–70, 2000.
Jeong, C. H., Hopke, P. K., Kim, E., and Lee, D. W.: The comparison between thermal-optical transmittance elemental carbon and aethalometer black carbon measured at multiple monitoring sites, Atmos. Environ., 38, 5193–5204, 2004.
Jimenez, J. L., Jayne, J. T., Shi, Q., Kolb, C. E., Worsnop, D. R., Yourshaw, I., Seinfeld, J. H., Flagan, R. C., Zhang, X., Smith, K. A., Morris, J. W., and Davidovits, P.: Ambient aerosol sampling using the aerodyne aerosol mass spectrometer, J. Geophys. Res., 108, 8425, doi:10.1029/2001JD001213, 2003.
Johnson, K. S., Zuberi, B., Molina, L. T., Molina, M. J., Iedema, M. J., Cowin, J. P., Gaspar, D. J., Wang, C., and Laskin, A.: Processing of soot in an urban environment: case study from the Mexico City Metropolitan Area, Atmos. Chem. Phys., 5, 3033–3043, doi:10.5194/acp-5-3033-2005, 2005.
Kittelson, D. B.: Engines and nanoparticles: a review, J. Aerosol Sci., 29, 575–588, 1998.
Knox, A., Evans, G. J., Brook, J. R., Yao, X., Jeong, C. H., Godri, K. J., Sabaliauskas, K., and Slowik, J. G.: Mass absorption cross-section of ambient black carbon aerosol in relation to chemical age, Aerosol Sci. Tech., 43, 522–532, 2009.
Lack, D. A. and Cappa, C. D.: Impact of brown and clear carbon on light absorption enhancement, single scatter albedo and absorption wavelength dependence of black carbon, Atmos. Chem. Phys., 10, 4207–4220, doi:10.5194/acp-10-4207-2010, 2010.
Lack, D. A., Lovejoy, E. R., Baynard, T., Pettersson, A., and Ravishankara, A. R.: Aerosol absorption measurement using photoacoustic spectroscopy: sensitivity, calibration, and uncertainty developments, Aerosol Sci. Tech., 40, 697–708, 2006.
Levy, I., Makar, P. A., Sills, D., Zhang, J., Hayden, K. L., Mihele, C., Narayan, J., Moran, M. D., Sjostedt, S., and Brook, J.: Unraveling the complex local-scale flows influencing ozone patterns in the Southern Great Lakes of North America, Atmos. Chem. Phys. Discuss., in press, 2010.
Lewis, K. A., Arnott, W. P., Moosmüller, H., Chakrabarty, R. K., Carrico, C. M., Kreidenweis, S. M., Day, D. E., Malm, W. C., Laskin, A., Jimenez, J. L., Ulbrich, I. M., Huffman, J. A., Onasch, T. B., Trimborn, A., Liu, L., and Mishchenko, M. I.: Reduction in biomass burning

ACPD
10, 19939–19980, 2010

aerosol light absorption upon humidification: roles of inorganically-induced hygroscopicity, particle collapse, and photoacoustic heat and mass transfer, Atmos. Chem. Phys., 9, 8949–8966, doi:10.5194/acp-9-8949-2009, 2009.

Liousse, C., Cachier, H., and Jennings, S. G.: Optical and thermal measurements of black carbon aerosol content in different environments: variation of the specific attenuation cross-section, Sigma, Atmos. Environ., 27A, 1203–1211, 1993.

Liu, L., Mishchenko, M. I., and Arnott, W. P.: A study of radiative properties of fractal soot aggregates using the superposition T-matrix method, J. Quant. Spectrosc. Ra., 109, 2656–2663, 2008.

Martins, J. V., Artaxo, P., Liousse, C., Reid, J. S., Hobbs, P. V., and Kaufman, Y. J.: Effects of black carbon content, particle size, and mixing on light absorption by aerosols from biomass burning in Brazil, J. Geophys. Res., 103, 32041–32050, 1998.

Mewes, B. and Seitzman, J. M.: Soot volume fraction and particle size measurements with laser-induced incandescence, Appl. Optics, 36, 709–717, 1997.

Moosmüller, H., Chakrabarty, R. K., and Arnott, W. P.: Aerosol light absorption and its measurements: a review, J. Quant. Spectrosc. Ra., 110, 844–878, 2009.

Moteki, N. and Kondo, Y.: Effects of mixing state on black carbon measurements by laser-induced incandescence, Aerosol Sci. Tech., 41, 398–417, 2007.

Murphy, D. M.: The effect of water evaporation on photoacoustic signals in transition and molecular flow, Aerosol Sci. Tech., 43, 356–363, 2009.

Pagels, J., Khalizov, A. F., McMurry, P. H., and Zhang, R. Y.: Processing of soot by controlled sulphuric acid and water condensation – mass and mobility relationship, Aerosol Sci. Tech., 43, 629–640, 2009.

Park, K., Cao, F., Kittelson, D. B., and McMurry, P. H.: Relationship between particle mass and mobility for diesel exhaust particles, Environ. Sci. Technol., 37, 577–583, 2003.

Ramachandran, G. and Reist, P. C.: Characterization of morphological changes in agglomerates subject to condensation and evaporation using multiple fractal dimension, Aerosol Sci. Tech., 23, 431–442, 1995.

Raspet, R., Hickey, C. J., and Sabatier, J. M.: The effect of evaporation-condensation on sound progatation in cylindrical tubes using the low reduced frequency approximation, J. Acoust. Soc. Am., 105, 65–73, 1999.

Raspet, R., Slaton, W. V., Arnott, W. P., and Moosmüller, H.: Evaporation-condenation effects on resonant photoacoustic of volatile aerosols, J. Atmos. Ocean. Tech., 20, 685–695, 2003.

ACPD

10, 19939–19980, 2010

Schulz, C., Kock, B. F., Hofmann, M., Michelsen, H., Will, S., Bougie, B., Suntz, R., and Smallwood, G.: Laser-induced incandescence: recent trends and current questions, Appl. Phys. B-Lasers O., 83, 333–354, 2006.

Sharma, S., Brook, J. R., Cachier, H., Chow, J., Gaudenzi, A., and Lu, G.: Light absorption and thermal measurements of black carbon in different regions of Canada, J. Geophys. Res., 107(D24), 4771, doi:10.1029/2002JD002496, 2002.

Shiraiwa, M., Kondo, Y., Iwamoto, T., and Kita, K.: Amplification of light absorption of black carbon by organic coating, Aerosol Sci. Tech., 44, 46–54, 2010.

Slowik, J. G., Stainken, K., Davidovits, P., Williams, L. R., Jayne, J. T., Kolb, C. E., Worsnop, D. R., Rudich, Y., DeCarlo, P. F., and Jimenez, J. L.: Particle morphology and density characterization by combined mobility and aerodynamic diameter measurements. Part 2: application to combustion-generated soot aerosols as a function of fuel equivalence ratio, Aerosol Sci. Tech., 38, 1206–1222, 2004.

Slowik, J. G., Cross, E. S., Han, J. H., Davidovits, P., Onasch, T. B., Jayne, J. T., Williams, L. R., Canagaratna, M. R., Worsnop, D. R., Chakrabarty, R. K., Moosmüller, H., Arnott, W. P., Schwarz, J. P., Gao, R. S., Fahey, D. W., Kok, G. L., and Petzold, A.: An inter-comparison of instruments measuring black carbon content of soot particles, Aerosol Sci. Tech., 41, 295–314, 2007a.

Slowik, J. G., Cross, E. S., Han, J. H., Kolucki, J., Davidovits, P., Williams, L. R., Obasch, T. B., Jayne, J. T., Kolb, C. E., and Worsnop, D. R.: Measurements of morphology changes of fractal soot particles using coating and denuding experiments: implications for optical absorption and atmospheric lifetime, Aerosol Sci. Tech., 41, 734–750, 2007b.

Smallwood, G. J.: A critique of laser-induced incandescence for the measurement of soot, Ph.D. thesis, Cranfield University, Cranfield, UK, 204 pp., 2009.

Snelling, D. R., Smallwood, G. J., Campbell, I. G., Medlock, J. E., and Glder, Ö. L.: Development and application of laser induced incandescence (LII) as a diagnostic for soot particulate measurements, in: Proceeding of AGARD 90th Symposium of the propulsion and energetics panel on advanced non-intrusive instrumentation for propulsion engines, Brussels, Belgium, 20–24 October, 23-1 to 23-9, 1998.

Snelling, D. R., Smallwood, G. J., Sawchuk, R. A., Neill, W. S., Gareau, D., Clavel, D. J., Chippior, W. L., Liu, F., Glder, Ö. L., and Bachalo, W. D.: In-situ real-time characterization of particulate emissions from a diesel engine exhaust by laser-induced incandescence, SAE Technical Paper Series, 2000-01-1994, 2000.

ACPD

10, 19939–19980, 2010

Snelling, D. R., Smallwood, G. J., Liu, F., Gülder, Ö. L., and Bachalo, W. D.: A calibration-independent LII technique for soot measurement by detecting absolute light intensity, Appl. Optics, 44, 6773–6785, 2005.

Snyder, D. C. and Schauer, J. J.: An inter-comparison of two black carbon aerosol instruments and a semi-continuous elemental carbon instrument in the urban environment, Aerosol Sci. Tech., 41, 463–474, 2007.

Turpin, B. J., Cary, R. A., and Huntzicker, J. J.: An in situ, time-resolved analyzer for aerosol organic and elemental carbon, Aerosol Sci. Tech., 12, 161–171, 1990.

Wainner, R. T. and Seitzman, J. M.: Soot diagnostics using laser-induced incandescence in flames and exhaust flows, in Proceeding of American Institute of Aeronautics and Astronautics 37th Aerospace Sciences Meeting and Exhibit, Reno, NV, 11–14 January, #99-0640, 1999.

Xue, H., Khalizov, A. F., Wang, L., Zheng, J., and Zhang, R.: Effects of dicarboxylic acid coating on the optical properties of soot, Phys. Chem. Chem. Phys., 11, 7869–7875, 2009.

ACPD

10, 19939–19980, 2010

Table 1. Average values for various measure quantities presented in this work. Bold values represent the mean values while the standard deviations and the number of valid data points are included in brackets. The particle light absorption coefficient (B_{abs}) and scattering coefficient (B_{scat}) are measured from the photoacoustic spectrometer (PA). The primary particle size (PPS) and soot volume fraction are obtained with the laser-induced incandescence instrument (LII). The particle coating mass and the average percentage breakdown for the four major particle compositions are based on measurements from the aerosol mass spectrometer (AMS). PA:LII ratio and specific attenuation coefficient (SAC) are the calculated values based on the individual pairs of B_{abs} and SVF measurements. The data resolution indicates the time resolution of the AMS data and the PA and LII measurements have been averaged to match accordingly.

Instrument	Measure quantity	Site location: Toronto (suburban)	Ottawa (street canyon)	Ottawa (near highway)	Windsor (in/out of city)
PA	B_{abs} $(Mm)^{-1}$	2.7 (SD=1.7, N=160)	20.0 (SD=15.8, N=29)	6.2 (SD=8.8, N=27)	1.1 (SD=1.6, N=1527)
PA	B_{scat} $(Mm)^{-1}$	9.9 (SD=7.4, N=160)	14.7 (SD=16.8, N=29)	13.0 (SD=5.1, N=27)	2.3 (SD=1.5, N=1527)
LII	PPS (nm)	27.4 (SD=10.7, N=141)	50.4 (SD=4.6, N=29)	66.2 (SD=7.0, N=27)	74.0 (SD=14.2, N=1688)
LII	SVF (ppt)	0.06 (SD=0.03, N=141)	0.9 (SD=0.4, N=29)	0.4 (SD=0.4, N=27)	0.2 (SD=0.3, N=1688)
AMS	Coating mass (%)	6.2 (SD=12.6, N=145)	11.2 (SD=3, N=29)	12.5 (SD=3, N=27)	12.5 (SD=16, N=1519)
AMS	Sulphate mass (%)	15 (SD=8.6, N=145)	8 (SD=2, N=29)	9 (SD=2, N=27)	24 (SD=12, N=1519)
AMS	Ammonium mass (%)	13 (SD=4.5, N=145)	4 (SD=1, N=29)	5 (SD=1, N=27)	11 (SD=5, N=1519)
AMS	Nitrate mass (%)	3 (SD=2.5, N=145)	3 (SD=1, N=29)	3 (SD=1, N=27)	5 (SD=3, N=1519)
PA+LII	PA:LII ratio (10^6) $(Mm)^{-1}$	42.7 (SD=16.8, N=141)	21.3 (SD=10.1, N=29)	12.3 (SD=7.8, N=27)	5.0 (SD=2.6, N=1520)
PA+LII	PA:LII (normalized) (10^6) $(Mm)^{-1}$ $(\mu g\,m^{-3})^{-1}$	10.0 (SD=6.8, N=141)	1.9 (SD=0.9, N=29)	1.0 (SD=0.6, N=27)	0.5 (SD=0.4, N=1512)
PA+LII	SAC $(m^2\,g^{-1})$	22.5 (SD=8.8, N=141)	11.2 (SD=5.4, N=29)	6.5 (SD=4.1, N=27)	2.6 (SD=1.4, N=1520)
AMS	Data resolution (min)	5	5	5	2, 5, 10, 15

ACPD
10, 19939–19980, 2010

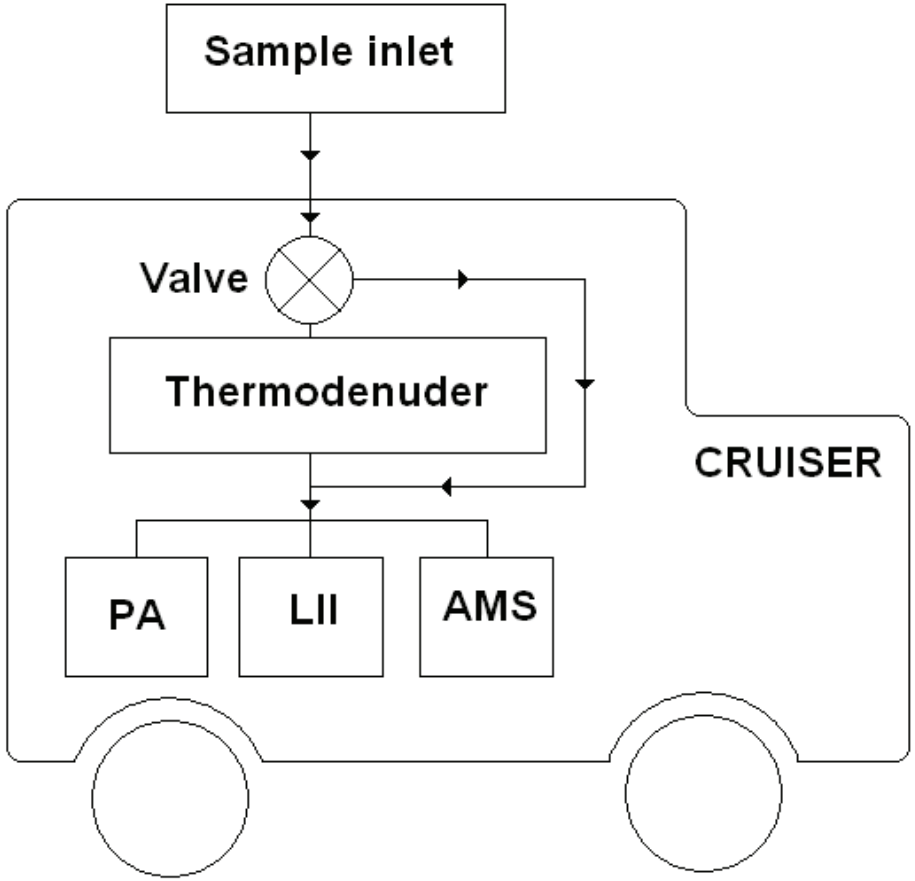

Fig. 1. Flow diagram for the thermodenuder experiment.

ACPD
10, 19939–19980, 2010

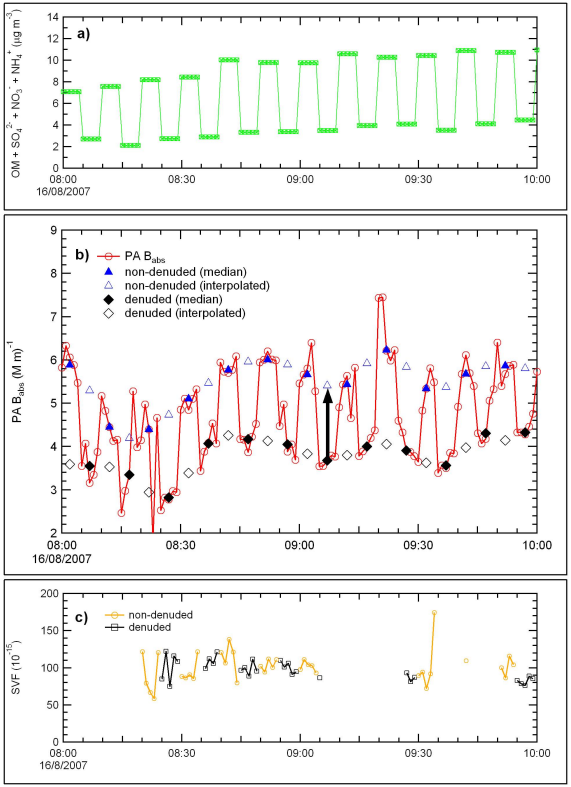

Fig. 2. Variations of **(a)** the particle coating mass measured by the AMS during the thermodenuder experiment for a 2-h period on 16 August 2007, **(b)** the particle light absorption (B_{abs}) measured by the photoacoustic spectrometer during the same period (red marker with line), the median and interpolated B_{abs} during non-denuded (blue solid and open triangles) and denuded (black solid and open diamonds) conditions, and **(c)** the soot volume fraction measured by the laser-induced incandescence instrument during the same period.

ACPD
10, 19939–19980, 2010

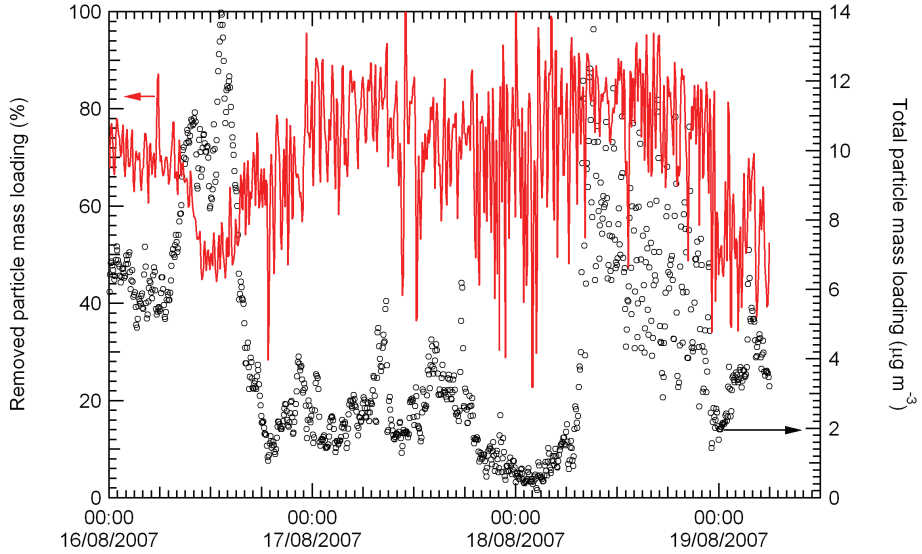

Fig. 3. The variations of the particle coating mass as determined by the AMS (black markers) over the course of the thermodenuder experiment and its corresponding percentage of removal of the particle coating mass (red line) on the particles.

ACPD
10, 19939–19980, 2010

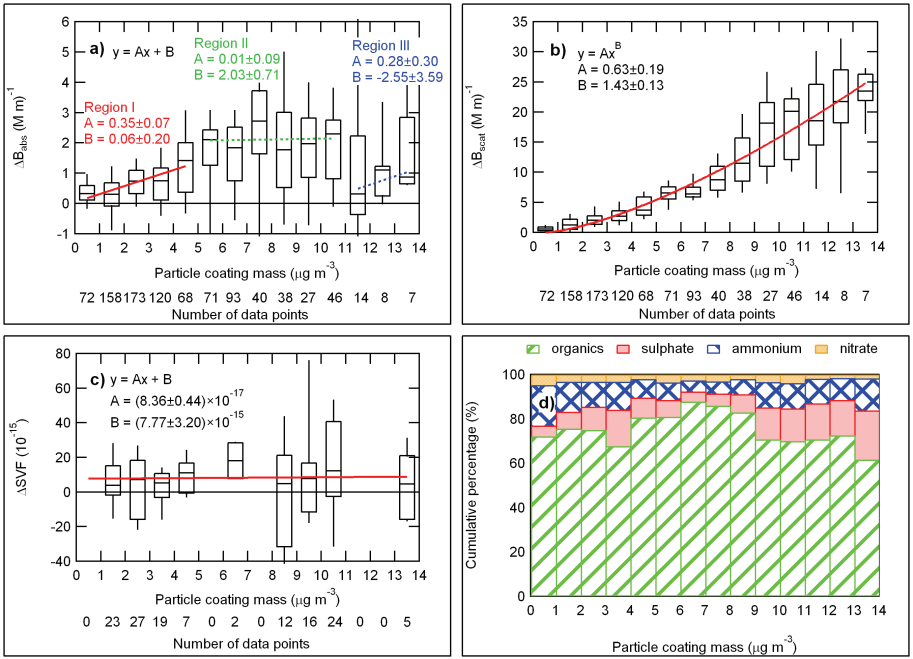

Fig. 4. The variations of the enhancement of **(a)** the particle light absorption, **(b)** particle light scattering, and **(c)** the soot volume fraction, as a function of particle coating mass measured at Toronto. The numbers in the lower bottom axis in panels (a) to (c) indicate the total number of valid data points. Figure 4d shows the relative contributions from organics, sulphate, ammonium, and nitrate within the coating mass at different stages during the thermodenuder experiment.

ACPD
10, 19939–19980, 2010

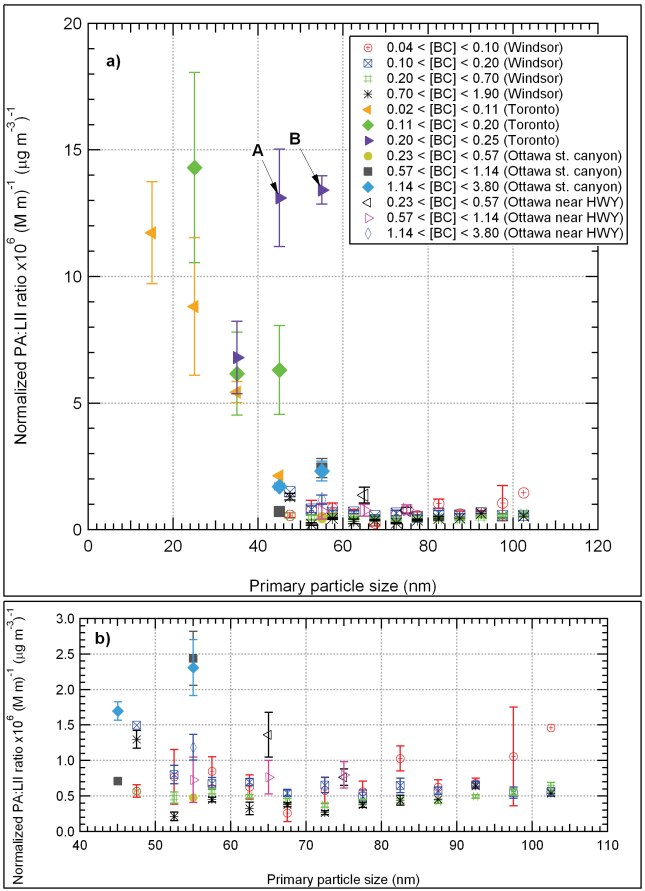

Fig. 5. Variations in the normalized PA:LII ratio as a function of primary particle size measured for **(a)** all field measurements (undenuded) and **(b)** all measurements except Toronto data. Error bars in the upper panel are the standard deviation of the mean.

ACPD
10, 19939–19980, 2010

Measurements of black carbon light absorption enhancement

T. W. Chan et al.

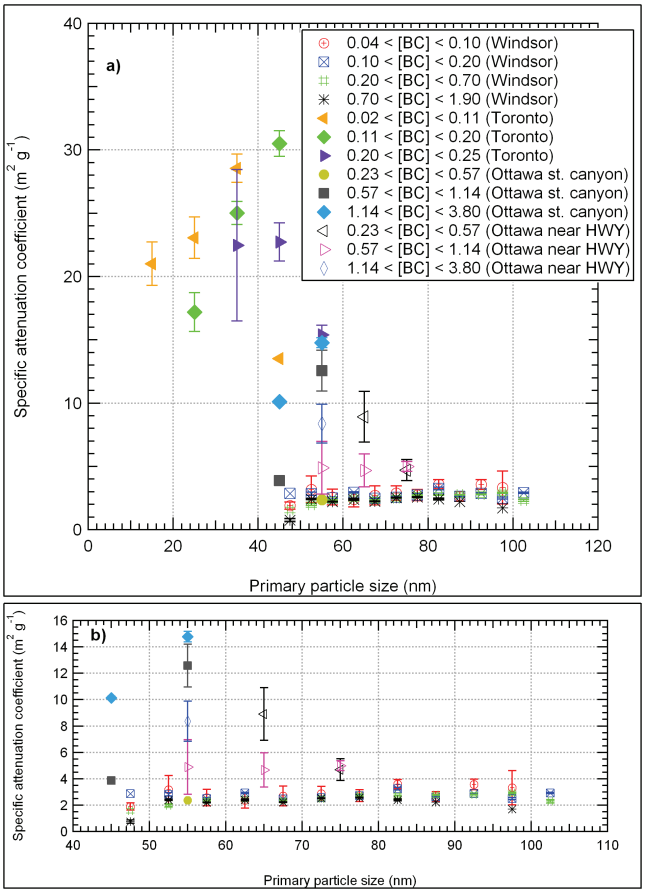

Fig. 6. The variations of the SAC as a function of primary particle size measured for **(a)** all field measurements (undenuded) and **(b)** all measurements except Toronto data. Error bars in the upper panel are standard deviation of the mean.

ACPD
10, 19939–19980, 2010